Supplement of Atmos. Chem. Phys., 25, 12451–12465, 2025
https://doi.org/10.5194/acp-25-12451-2025-supplement


Atmospheric Chemistry and Physics
Open Access
EGU

*Supplement of*

# The critical role of volatile organic compound emissions in nitrate formation in Lhasa, Tibetan Plateau: insights from oxygen isotope anomaly measurements

**Xueqin Zheng et al.**

*Correspondence to:* Junwen Liu (liu.junwen@jnu.edu.cn)

**Text S1. nitrate ($NO_3^-$) formation pathways**

In the atmosphere, $NO_3^-$ is primarily produced via the oxidation of nitrogen oxides ($NO_x$ =NO + $NO_2$). NO, emitted from various sources, rapidly enters the $NO_x$ cycle, where it is converted into $NO_2$. This $NO_2$ is then oxidized to form $NO_3^-$ via three main pathways. During the daytime, OH radicals oxidize $NO_2$ to form $HNO_3$ (g) ($NO_2$ + OH), a process that predominates under conditions of strong photochemistry and elevated temperature. Additionally, $NO_2$ can react with $O_3$ to form $NO_3$ radicals, which subsequently reacts with volatile organic compound (VOC) or dimethylsulfide (DMS) to produce $HNO_3$ (g) ($NO_3$ + VOC/DMS), with the $NO_3$ + DMS reaction occurring mainly in coastal areas (Heintz et al., 1996; Brown et al., 2011). This reaction takes place predominantly at night, as $NO_3$ radical are easily photolyzed back to $NO_2$ in sunlight. Moreover, $NO_3$ can react with atmospheric $NO_2$ to form dinitrogen pentoxide ($N_2O_5$), which hydrolyzes on the surface of the aerosol to form liquid $HNO_3$ ($N_2O_5$ + $H_2O$). The produced liquid or gaseous $HNO_3$ further reacts with alkaline gases such as $NH_3$ to form $NO_3^-$ (Zheng et al., 2015; Cao et al., 2022).

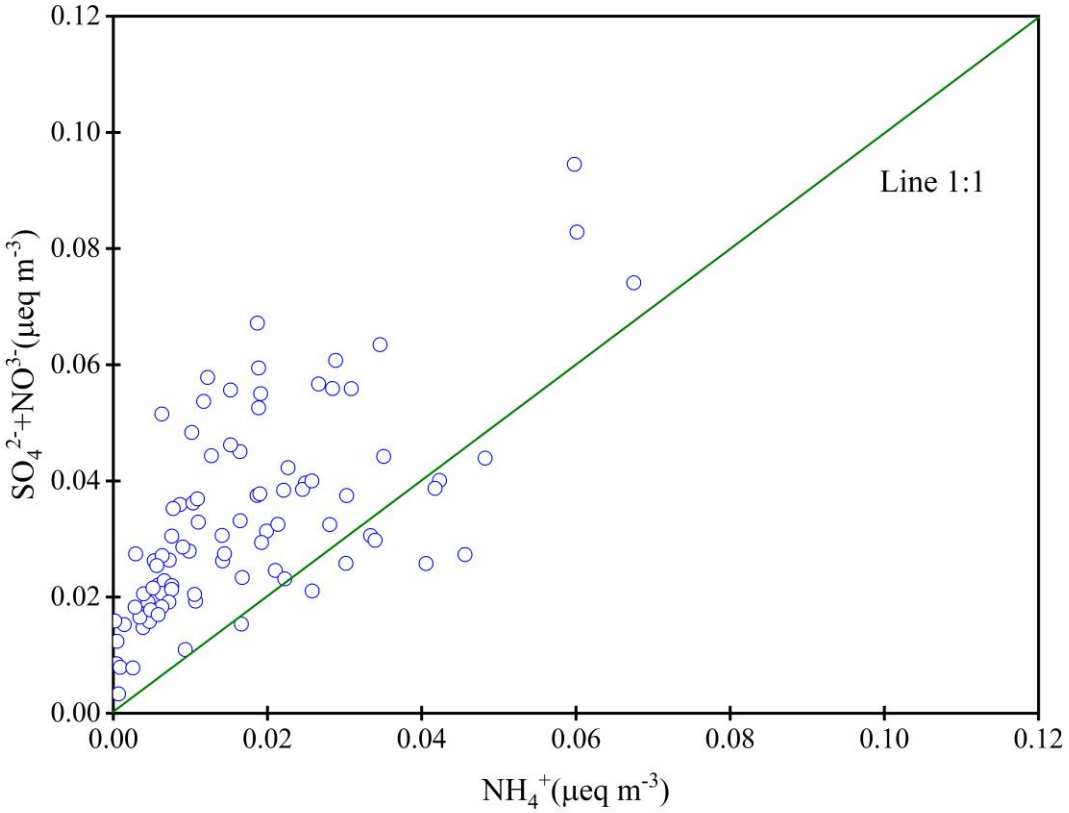


*Figure S1 Equivalent concentrations of $SO_4^{2-}+NO_3^{-}/NH_4^{+}$ in Lhasa during the sampling campaign.*

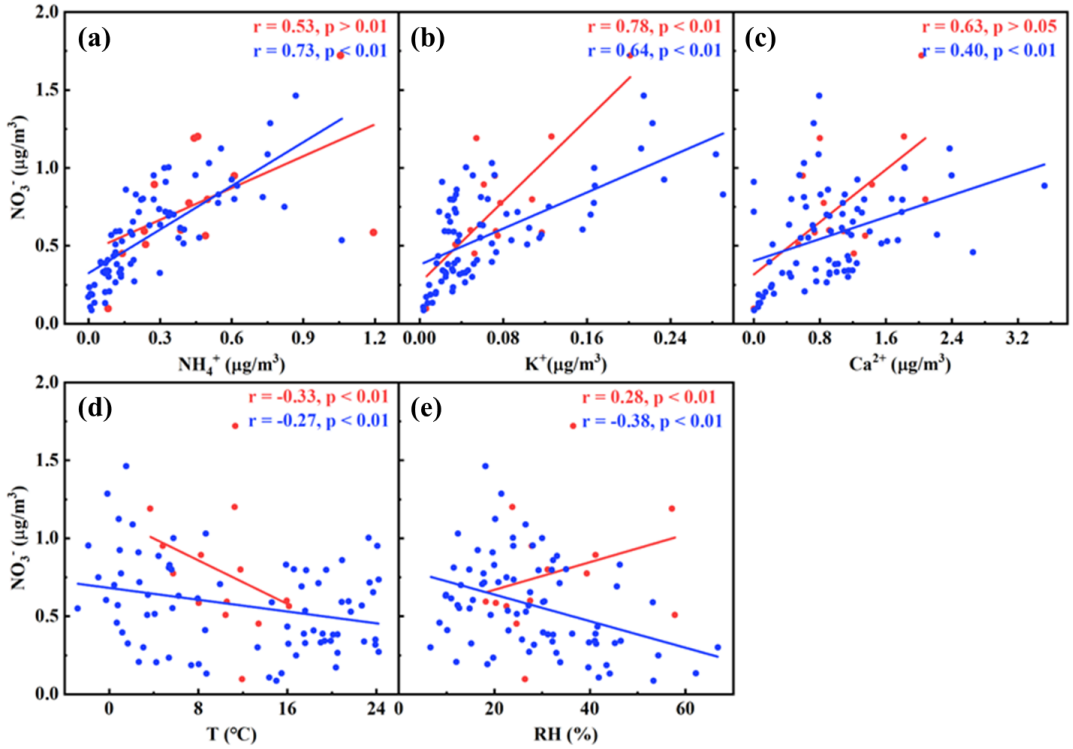


*Figure S2 Relationships between $NO_3^-$ and other parameters. The relationship between $NO_3$ concentrations and (a) $NH_4^+$ concentrations, (b) $K^+$ concentrations, (c) $Ca^{2+}$concentrations, (d) T, and (e) RH. The red and blue represent spring and other seasons, respectively.*

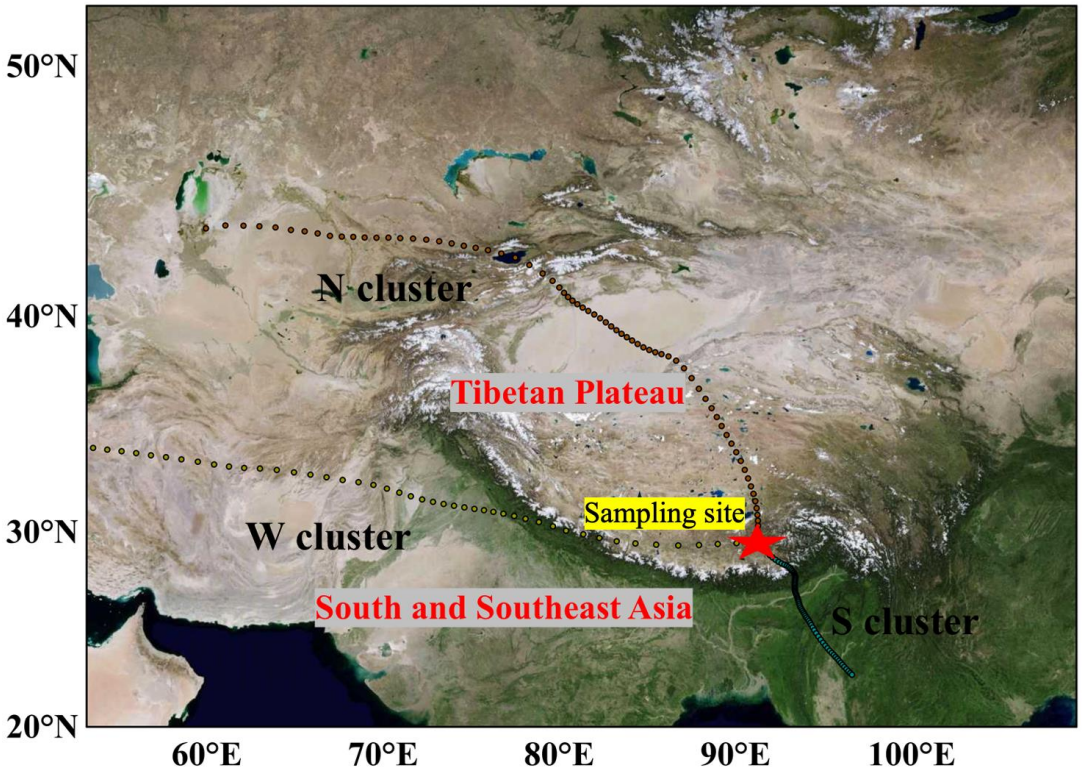


*Figure S3. The air clusters of backward trajectories in Lhasa during the sampling campaign. The red star denotes the sampling site.*

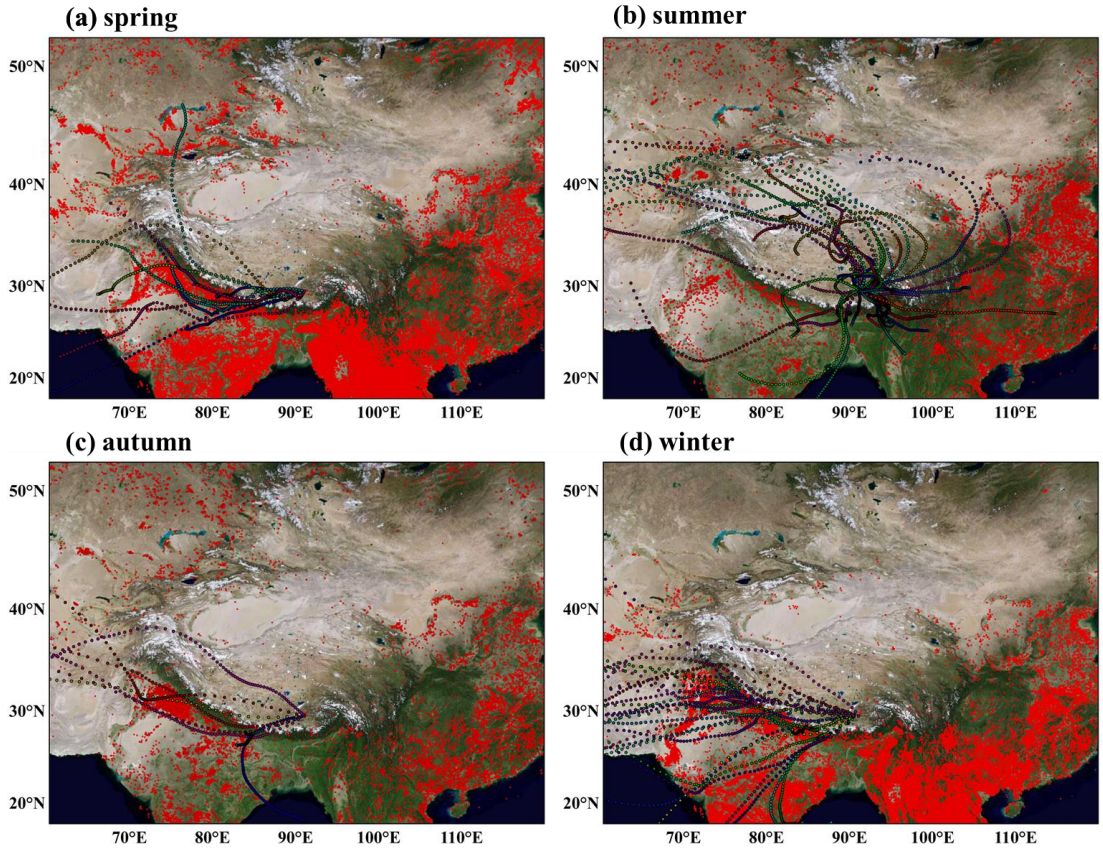


*Figure S4. Back trajectories using HYSPLIT model in (a) spring, (b) summer, (c) autumn, and (d) winter. The red dots are fire spots observed by the MODIS and originated from https://firms.modaps.eosdis.nasa.gov/download/.*

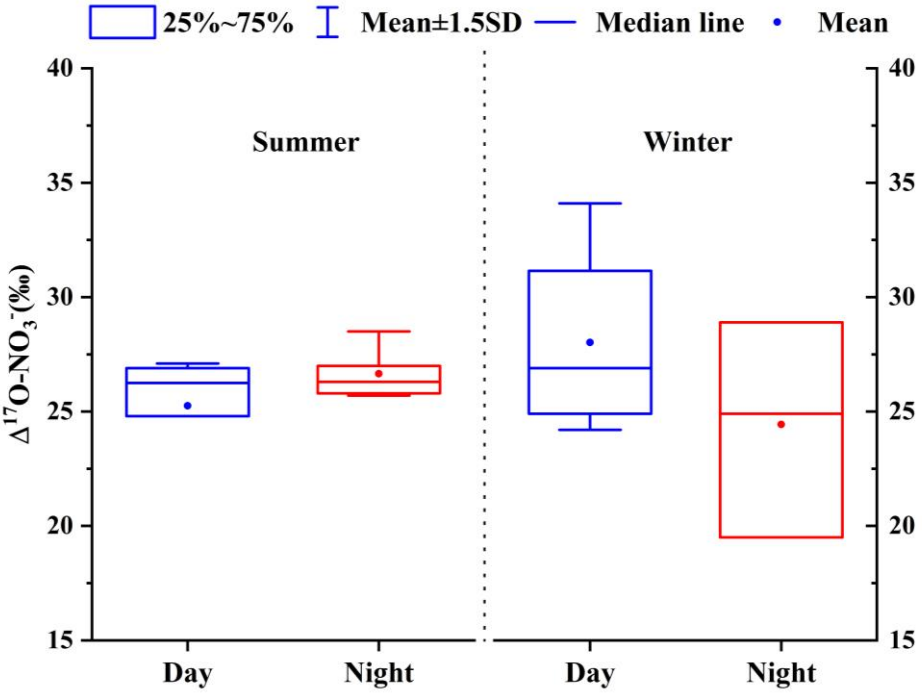


*Figure S5 Diurnal variation of $\Delta^{17}O\text{-}NO_3^-$ values in summer and winter during the sampling campaign.*

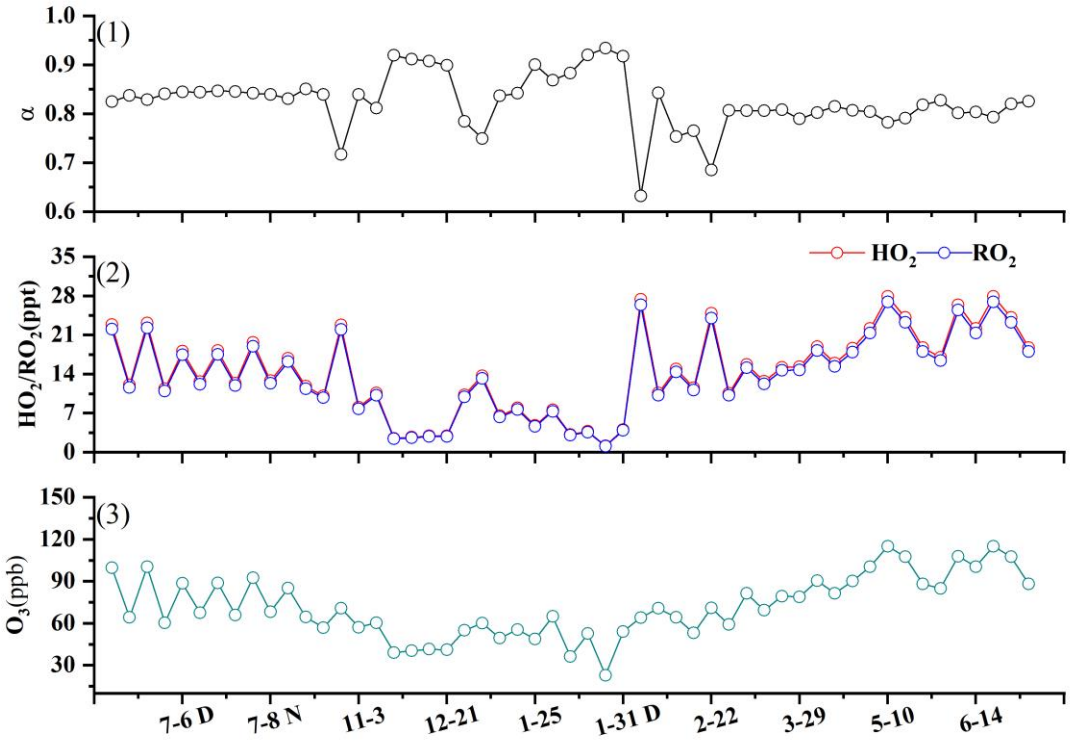


*Figure S6 Time series of (1) a value; (2) $HO_2$ and $RO_2$ concentrations; and (3)$O_3$ concentrations during the sampling campaign. The volume mixing ratios were calculated from mass concentrations (μg/m$^3$) based on the local atmospheric pressure and temperature conditions in Lhasa.*

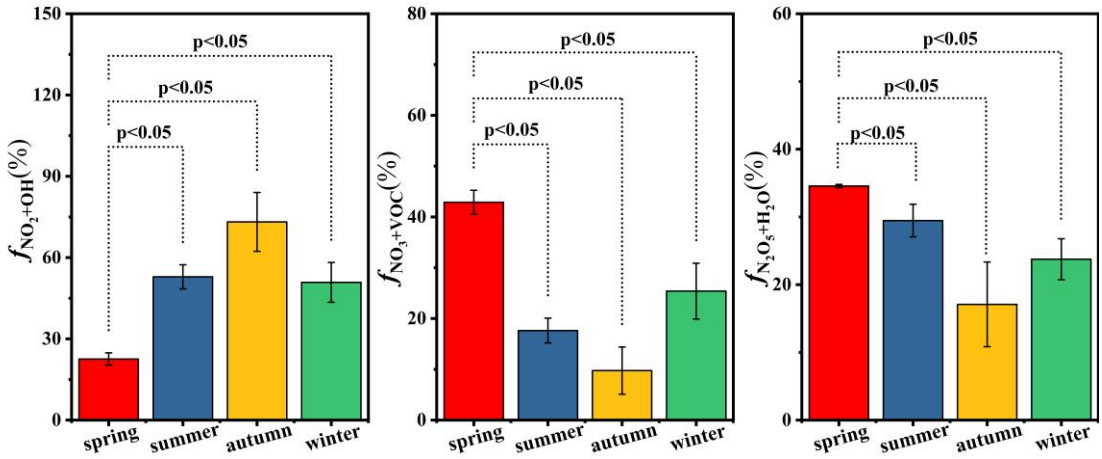


*Figure S7 Seasonal variations in average contributions and statistical significance.*

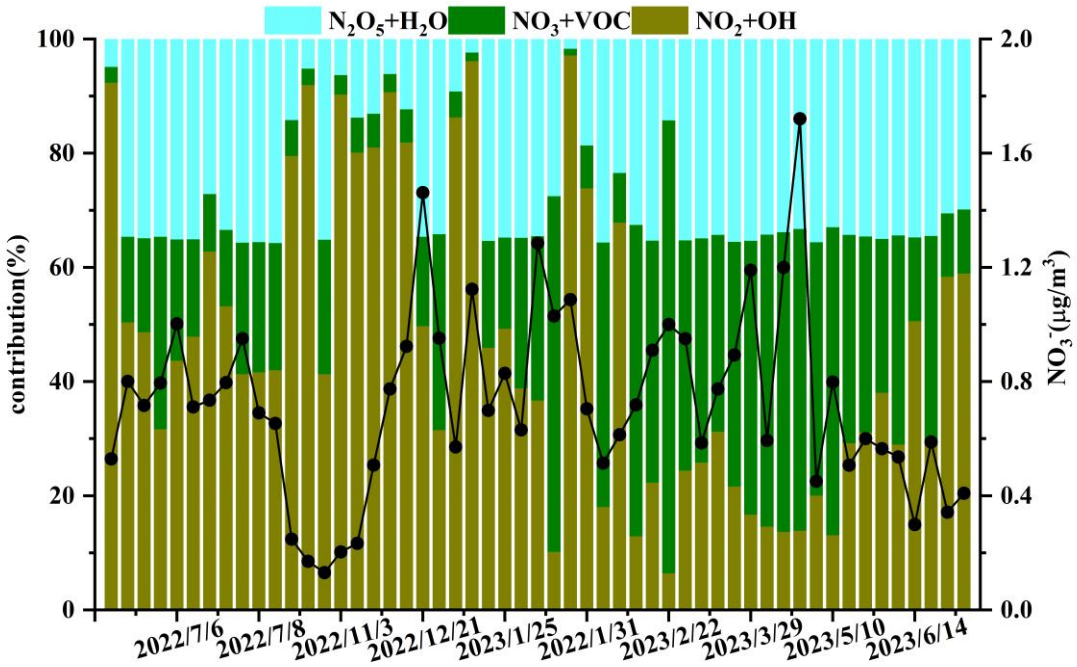


*Figure S8. Time series of $NO_3^-$ concentrations (black line) and the relative contributions of three pathways ($NO_2$ + OH, $NO_3$ + VOC and $N_2O_5$ + $H_2O$) to $NO_3^-$ formation in Lhasa during the sampling campaign.*

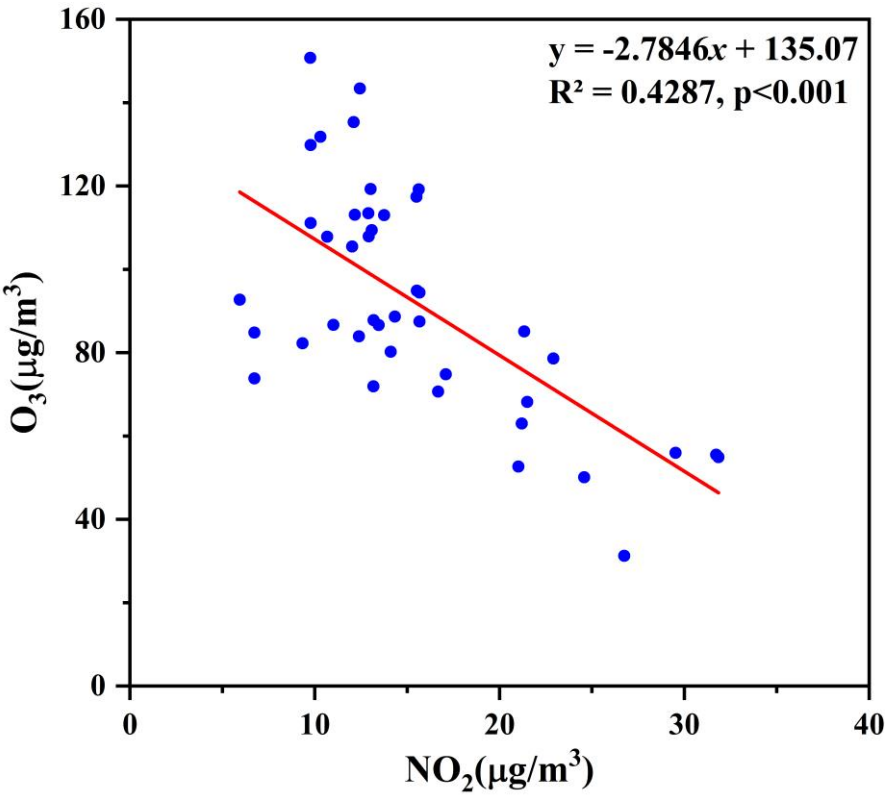


*Figure S9 The relationship between atmospheric $NO_2$ concentrations and $O_3$ concentrations in Lhasa during the sampling campaign.*

Table S1 Average diurnal variations of WSIs and $\Delta^{17}O\text{-}NO_3^-$ during summer and winter sampling campaign

| Target | Unit | Summer | | Winter | |
|---|---|---|---|---|---|
| | | Daytime | Nightttime | Daytime | Nightttime |
| $Na^+$ | μg/m$^3$ | 0.16 ± 0.14 | 0.09 ± 0.03 | 0.09 ± 0.08 | 0.09 ± 0.05 |
| $NH_4^+$ | μg/m$^3$ | 0.30 ± 0.26 | 0.52 ± 0.30 | 0.18 ± 0.17 | 0.04 ± 0.04 |
| $K^+$ | μg/m$^3$ | 0.07 ±0.06 | 0.09 ± 0.04 | 0.03 ± 0.02 | 0.03 ± 0.03 |
| $Mg^{2+}$ | μg/m$^3$ | 0.02 ± 0.01 | 0.02 ± 0.01 | 0.02 ± 0.01 | 0.02 ± 0.01 |
| $Ca^{2+}$ | μg/m$^3$ | 1.09 ± 0.70 | 1.67 ± 0.51 | 1.15 ± 0.50 | 0.13 ± 0.08 |
| $Cl^-$ | μg/m$^3$ | 0.08 ± 0.10 | 0.03 ± 0.01 | 0.03 ± 0.03 | 0.05 ± 0.05 |
| $NO_3^-$ | μg/m$^3$ | 0.60 ± 0.31 | 0.83 ± 0.35 | 0.50 ± 0.23 | 0.23 ± 0.13 |
| $SO_4^{2-}$ | μg/m$^3$ | 0.74 ± 0.45 | 1.11 ± 0.52 | 0.72 ± 0.45 | 0.31 ± 0.14 |
| T | ℃ | 23.4 ± 0.83 | 18.0 ± 1.04 | 8.21 ± 1.34 | 2.01 ± 1.73 |
| RH | % | 24.0 ± 3.06 | 35.1 ± 5.60 | 12.6 ± 2.93 | 24.3 ± 2.10 |
| $NO_2$ | μg/m$^3$ | 12.9 ± 1.61 | 19.2 ± 3.52 | 14.7 ± 1.54 | 20.8 ± 6.97 |
| $O_3$ | μg/m$^3$ | 118 ± 7.61 | 84.7 ± 3.52 | 81.2 ± 10.2 | 56.0 ± 23.0 |
| $\Delta^{17}O\text{-}NO_3\text{-}$ | ‰ | 25.3 ± 2.39 | 26.7 ± 1.02 | 28.0 ± 3.79 | 24.4 ± 3.85 |

Table S2 Comparison of average values of $\Delta^{17}O\text{-}NO_3^-$ in Lhasa with other cities

| Sampling site | Altitude(m) | Sample | Sampling period | $\Delta^{17}O\text{-}NO_3^-$(‰) | Reference |
|---|---|---|---|---|---|
| Lhasa | 3650 | $PM_{2.5}$ | June, 2022-<br>July, 2023 | 26.3 ± 3.13 | this study |
| Himalayan-Tibetan Plateau | 4276 | TSP | April 2018-September 2018 | 24.1 ± 3.9 | (Xia et al., 2019) |
| Mt.Lulin Taiwan | 2862 | TSP | April 2021-September 2021 | 16.3 ± 6.5 | (Guha et al., 2017) |
| Uinta Mountain | 1281-3486 | snow | May July, August 2009<br>April 2011 | 23.7 ± 5.6 | (Hundey et al., 2016) |
| French Antarctic Station Dumont d'Urville | 40 | —— | January 2001-December 2001 | 31.4 ± 6.2 | (Savarino et al., 2007) |
| Alert, Nunavut, Canada | 190 | —— | March 2004-May,2004 | 32.7 ± 1.7 | (Morin et al., 2007) |
| Trinidad Head, a coastal site of northern California | 107 | TSP | March 2002-May 2002 | 24.8 ± 2.0 | (Patris et al., 2007) |
| Nanjing | —— | $PM_{2.5}$ | January 2015 | 30.5 | (Zhang et al., 2022) |
| Shanghai | —— | $PM_{2.5}$ | January 2016-June 2016 | 20.5-31.9 | (He et al., 2020) |
| Beijing | —— | $PM_{2.5}$ | November 2016 -December, 2016<br>May 2017-June 2017 | Winter: 29.0 ± 1.0<br>Summer: 27.3 ± 2.4 | (Fan et al., 2021) |
| Guangzhou | —— | $PM_{2.5}$ | October 2018-November 2018 | 25.0 ± 1.39 | (Wang et al., 2023) |

Table S3 The average contribution of three oxidation pathways to $NO_3^-$ formation for the different the α values and $\Delta^{17}O\text{-}O_3$* values

| parameters | relative contribution of different oxidation pathways (%) | | |
|---|---|---|---|
| | **$NO_2$+OH** | **$NO_3$+VOC** | **$N_2O_5$+$H_2O$** |
| $\Delta^{17}O\text{-}O_3^*$=39‰ | | | |
| α=0.7 | 25 | 47 | 28 |
| α=0.8 | 41 | 29 | 30 |
| α=0.9 | 46 | 26 | 28 |
| α=0.68-0.93 | | | |
| $\Delta^{17}O\text{-}O_3$*=37‰ | 37 | 35 | 28 |
| $\Delta^{17}O\text{-}O_3$*=38‰ | 42 | 30 | 28 |
| $\Delta^{17}O\text{-}O_3$*=39‰ | 46 | 26 | 28 |

Table S4 Comparison of the relative contributions of three pathways to $NO_3^-$ formation in Lhasa and other cities

| Sampling site | Latitude and longitude | Sampling period | Season | Day and night | $f_{NO2+OH}$(%) | $f_{NO3+VOC}$(%) | $f_{N2O5+H2O}$(%) | Reference |
|---|---|---|---|---|---|---|---|---|
| Nanjing | 32°12′N, 118°44′E | 2015 | winter | | 38 | 27 | 35 | (Zhang et al., 2022) |
| | | | winter | | 44 | 22 | 34 | |
| | | | | | 39 | 25 | 36 | |
| Himalayan-Tibetan Plateau | 28.36°N, 86.95°E | 2017 | spring | | 35 | 4 | 62 | (Lin et al., 2021) |
| | | 2017 | summer | | 79 | 4 | 17 | |
| | | 2017 | autumn | | 77 | 4 | 19 | |
| | | 2017/2018 | winter | | 58 | 4 | 38 | |
| | | 2017/2018 | annual | | 43 | 5 | 52 | |
| Shenyang | 41.77°N, 123.43°E | 2016/2017/2018 | spring | | 66 | 9 | 25 | (Li et al., 2022) |
| | | 2016/2017/2018 | summer | | 95 | 2 | 3 | |
| | | 2016/2017/2018 | autumn | | 82 | 6 | 13 | |
| | | 2016/2017/2018 | winter | | 58 | 13 | 29 | |
| | | 2016 | annual | | 91 | 3 | 6 | |
| | | 2017 | annual | | 76 | 7 | 17 | |
| | | 2018 | annual | | 84 | 5 | 11 | |
| Qingyuan | 41.85°N, 124.94°E | 2015/2016/2017 | spring | | 40 | 25 | 35 | (Li et al., 2022) |
| | | 2015/2016/2017 | summer | | 85 | 5 | 10 | |
| | | 2015/2016/2017 | autumn | | 46 | 18 | 36 | |
| | | 2015/2016/2017 | winter | | 37 | 28 | 35 | |
| | | 2015 | annual | | 62 | 10 | 28 | |
| | | 2016 | annual | | 47 | 17 | 36 | |
| | | 2017 | annual | | 57 | 12 | 31 | |
| Beijing | 40°04′N, 116°42′E | 2014 | spring | | 27 | 38 | 35 | (Wang et al., 2019) |
| | | | summer | | 41 | 23 | 36 | |

| | | | | | | | | |
|---|---|---|---|---|---|---|---|---|
| | | | autumn | | 25 | 40 | 35 | |
| | | | winter | | 32 | 34 | 34 | |
| | | | annual | | 32 | 34 | 34 | |
| Beijing | 40.41° N, 116.68° E | 2015 | winter | daytime | 31 | 34 | 35 | (He et al., 2018) |
| | | | | nighttime | 28 | 37 | 35 | |
| Beijing | 39°58′ N, 116°22′E | 2017 | summer | | 46 | 31 | 23 | (Fan et al., 2021) |
| | | 2016 | winter | | 43 | 32 | 25 | |
| | | 2023 | spring | | 23 | 43 | 34 | |
| | | 2022/2023 | summer | | 53 | 18 | 29 | |
| | | 2022 | autumn | | 73 | 10 | 17 | |
| | | 2022/2023 | winter | | 51 | 25 | 24 | |
| Lhasa | 29.40°N, 91.08°E | | summer | daytime | 55 | 16 | 29 | this study |
| | | | | nighttime | 45 | 20 | 35 | |
| | | | winter | daytime | 48 | 26 | 26 | |
| | | | | nighttime | 51 | 25 | 24 | |
| | | 2022/2023 | annual | | 46 | 26 | 28 | |
| Guangzhou | 113.3°E, 23.1°N | 2018 | autumn | | 61 | 12 | 27 | (Wang et al., 2023) |

**Reference**

Alexander, B., Hastings, M., Allman, D., Dachs, J., Thornton, J., and Kunasek, S.: Quantifying atmospheric nitrate formation pathways based on a global model of the oxygen isotopic composition ($\Delta^{17}O$) of atmospheric nitrate, Atmospheric Chemistry and Physics, 9, 5043-5056, https://doi.org/10.5194/acp-9-5043-2009, 2009.

Brown, S. S., Dubé, W. P., Peischl, J., Ryerson, T. B., Atlas, E., Warneke, C., de Gouw, J. A., te Lintel Hekkert, S., Brock, C. A., Flocke, F., Trainer, M., Parrish, D. D., Feshenfeld, F. C., and Ravishankara, A. R.: Budgets for nocturnal VOC oxidation by nitrate radicals aloft during the 2006 Texas Air Quality Study, Journal of Geophysical Research: Atmospheres, 116, https://doi.org/10.1029/2011JD016544, 2011.

Cao, Y., Ma, Q., Chu, B., and He, H.: Homogeneous and heterogeneous photolysis of nitrate in the atmosphere: state of the science, current research needs, and future prospects, Frontiers of Environmental Science & Engineering, 17, 48, https://doi.org/10.1007/s11783-023-1648-6, 2022.

Fan, M.-Y., Zhang, Y.-L., Lin, Y.-C., Hong, Y., Zhao, Z.-Y., Xie, F., Du, W., Cao, F., Sun, Y., and Fu, P.: Important role of $NO_3$ radical to nitrate formation aloft in urban Beijing: Insights from triple oxygen isotopes measured at the tower, Environmental Science & Technology, 56, 6870-6879, https://doi.org/10.1021/acs.est.1c02843, 2021.

Guha, T., Lin, C., Bhattacharya, S., Mahajan, A., Ou-Yang, C.-F., Lan, Y.-P., Hsu, S., and Liang, M.-C.: Isotopic ratios of nitrate in aerosol samples from Mt. Lulin, a high-altitude station in Central Taiwan, Atmospheric Environment, 154, 53-69, https://doi.org/10.1016/j.atmosenv.2017.01.036, 2017.

He, P., Xie, Z., Yu, X., Wang, L., Kang, H., and Yue, F.: The observation of isotopic compositions of atmospheric nitrate in Shanghai China and its implication for reactive nitrogen chemistry, Science of the Total Environment, 714, 136727, https://doi.org/10.1016/j.scitotenv.2020.136727, 2020.

He, P., Xie, Z., Chi, X., Yu, X., Fan, S., Kang, H., Liu, C., and Zhan, H.: Atmospheric

$\Delta^{17}O(NO_3^-)$ reveals nocturnal chemistry dominates nitrate production in Beijing haze, Atmospheric Chemistry and Physics, 18, 14465-14476, https://doi.org/10.5194/acp-18-14465-2018, 2018.

Heintz, F., Platt, U., Flentje, H., and Dubois, R.: Long-term observation of nitrate radicals at the Tor Station, Kap Arkona (Rügen), Journal of Geophysical Research: Atmospheres, 101, 22891-22910, https://doi.org/10.1029/96JD01549, 1996.

Hundey, E. J., Russell, S., Longstaffe, F. J., and Moser, K. A.: Agriculture causes nitrate fertilization of remote alpine lakes, Nature Communications, 7, 10571, https://doi.org/10.1038/ncomms10571, 2016.

Ishino, S., Hattori, S., Savarino, J., Jourdain, B., Preunkert, S., Legrand, M., Caillon, N., Barbero, A., Kuribayashi, K., and Yoshida, N.: Seasonal variations of triple oxygen isotopic compositions of atmospheric sulfate, nitrate, and ozone at Dumont d'Urville, coastal Antarctica, Atmospheric Chemistry and Physics, 17, 3713-3727, https://doi.org/10.5194/acp-17-3713-2017, 2017.

Kanaya, Y., Cao, R., Akimoto, H., Fukuda, M., Komazaki, Y., Yokouchi, Y., Koike, M., Tanimoto, H., Takegawa, N., and Kondo, Y.: Urban photochemistry in central Tokyo: 1. Observed and modeled OH and $HO_2$ radical concentrations during the winter and summer of 2004, Journal of Geophysical Research: Atmospheres, 112, https://doi.org/10.1029/2007JD008670, 2007.

Kunasek, S., Alexander, B., Steig, E., Hastings, M., Gleason, D., and Jarvis, J.: Measurements and modeling of $\Delta^{17}O$ of nitrate in snowpits from Summit, Greenland, Journal of Geophysical Research: Atmospheres, 113, https://doi.org/10.1029/2008JD010103, 2008.

Li, Z., Walters, W. W., Hastings, M. G., Song, L., Huang, S., Zhu, F., Liu, D., Shi, G., Li, Y., and Fang, Y.: Atmospheric nitrate formation pathways in urban and rural atmosphere of Northeast China: Implications for complicated anthropogenic effects, Environmental Pollution, 296, 118752, https://doi.org/10.1016/j.envpol.2021.118752, 2022.

Lin, Y.-C., Zhang, Y.-L., Yu, M., Fan, M.-Y., Xie, F., Zhang, W.-Q., Wu, G., Cong, Z., and Michalski, G.: Formation mechanisms and source apportionments of airborne

nitrate aerosols at a Himalayan-Tibetan Plateau site: Insights from nitrogen and oxygen isotopic compositions, Environmental Science & Technology, 55, 12261-12271, https://doi.org/10.1021/acs.est.1c03957, 2021.

Michalski, G., Scott, Z., Kabiling, M., and Thiemens, M. H.: First measurements and modeling of $\Delta^{17}O$ in atmospheric nitrate, Geophysical Research Letters, 30, 2003.

Morin, S., Savarino, J., Bekki, S., Gong, S., and Bottenheim, J.: Signature of Arctic surface ozone depletion events in the isotope anomaly ($\Delta^{17}O$) of atmospheric nitrate, Atmospheric Chemistry and Physics, 7, 1451-1469, https://doi.org/10.5194/acp-7-1451-2007, 2007.

Patris, N., Cliff, S., Quinn, P., Kasem, M., and Thiemens, M.: Isotopic analysis of aerosol sulfate and nitrate during ITCT-2k2: Determination of different formation pathways as a function of particle size, Journal of Geophysical Research: Atmospheres, 112, https://doi.org/10.1029/2005JD006214, 2007.

Savarino, J., Kaiser, J., Morin, S., Sigman, D. M., and Thiemens, M. H.: Nitrogen and oxygen isotopic constraints on the origin of atmospheric nitrate in coastal Antarctica, Atmos. Chem. Phys., 7, 1925-1945, https://doi.org/10.5194/acp-7-1925-2007, 2007.

Savarino, J., Vicars, W. C., Legrand, M., Preunkert, S., Jourdain, B., Frey, M. M., Kukui, A., Caillon, N., and Gil Roca, J.: Oxygen isotope mass balance of atmospheric nitrate at Dome C, East Antarctica, during the OPALE campaign, Atmospheric Chemistry and Physics, 16, 2659-2673, https://doi.org/10.5194/acp-16-2659-2016, 2016.

Vicars, W. C. and Savarino, J.: Quantitative constraints on the $^{17}O$-excess ($\Delta^{17}O$) signature of surface ozone: Ambient measurements from 50 N to 50 S using the nitrite-coated filter technique, Geochimica et Cosmochimica Acta, 135, 270-287, https://doi.org/10.1016/j.gca.2014.03.023, 2014.

Vicars, W. C., Bhattacharya, S., Erbland, J., and Savarino, J.: Measurement of the $^{17}O$-excess ($\Delta^{17}O$) of tropospheric ozone using a nitrite-coated filter, Rapid Communications in Mass Spectrometry, 26, 1219-1231, https://doi.org/10.1002/rcm.6218, 2012.

Wang, Y., Liu, J., Jiang, F., Chen, Z., Wu, L., Zhou, S., Pei, C., Kuang, Y., Cao, F., and Zhang, Y.: Vertical measurements of stable nitrogen and oxygen isotope composition of fine particulate nitrate aerosol in Guangzhou city: Source apportionment and oxidation pathway, Science of The Total Environment, 865, 161239, https://doi.org/10.1016/j.scitotenv.2022.161239, 2023.

Wang, Y. L., Song, W., Yang, W., Sun, X. C., Tong, Y. D., Wang, X. M., Liu, C. Q., Bai, Z. P., and Liu, X. Y.: Influences of atmospheric pollution on the contributions of major oxidation pathways to $PM_{2.5}$ nitrate formation in Beijing, Journal of Geophysical Research: Atmospheres, 124, 4174-4185, https://doi.org/10.1029/2019JD030284, 2019.

Xia, X., Li, S., Wang, F., Zhang, S., Fang, Y., Li, J., Michalski, G., and Zhang, L.: Triple oxygen isotopic evidence for atmospheric nitrate and its application in source identification for river systems in the Qinghai-Tibetan Plateau, Science of the total environment, 688, 270-280, https://doi.org/10.1016/j.scitotenv.2019.06.204, 2019.

Zhang, Y.-L., Zhang, W., Fan, M.-Y., Li, J., Fang, H., Cao, F., Lin, Y.-C., Wilkins, B. P., Liu, X., and Bao, M.: A diurnal story of $\Delta^{17}O(NO_3^-)$ in urban Nanjing and its implication for nitrate aerosol formation, npj Climate and Atmospheric Science, 5, 50, https://doi.org/10.1038/s41612-022-00273-3, 2022.

Zheng, B., Zhang, Q., Zhang, Y., He, K., Wang, K., Zheng, G., Duan, F., Ma, Y., and Kimoto, T.: Heterogeneous chemistry: a mechanism missing in current models to explain secondary inorganic aerosol formation during the January 2013 haze episode in North China, Atmospheric Chemistry and Physics, 15, 2031-2049, https://doi.org/10.5194/acp-15-2031-2015, 2015.